J Solution Chem (2011) 40: 327–347
DOI 10.1007/s10953-010-9639-1

Effect of Solvents and pH on β-Cyclodextrin Inclusion Complexation of 2,4-Dihydroxyazobenzene and 4-Hydroxyazobenzene

J. Premakumari · G. Allan Gnana Roy · A. Antony Muthu Prabhu · G. Venkatesh · V.K. Subramanian · N. Rajendiran

Received: 2 March 2010 / Accepted: 27 July 2010 / Published online: 12 January 2011

Abstract The spectral characteristics of 2,4-dihydroxyazobenzene (DHAB, sudan orange G) and 4-hydroxyazobenzene (HAB) have been studied in various solvents, different hydrogen ion and β-cyclodextrin (β-CD) concentrations, and are compared with azobenzene (AB). The inclusion complexes of the above molecules with β-CD were analyzed by UV-vis spectrometry, flourometry, FT-IR, ^{1}H NMR, SEM and DFT methods. The solvent study shows that only the azo form is present in DHAB and HAB molecules. The unusually large red shift observed in acidic solutions indicates both molecules exhibit azo-hydrazo tautomerization. In the β-CD solutions, the increase in fluorescence intensity and large bathochromic shift in the S_1 state indicates that DHAB and HAB form 2:2 inclusion complexes, whereas AB forms a 1:1 inclusion complex.

Keywords 2,4-Dihydroxyazobenzene · Azo-hydrazo tautomerism · β-Cyclodextrin · Inclusion complex

1 Introduction

Electron transfer and proton transfer reactions are the most fundamental problems in photochemistry. In recent years, there has been tremendous interest in studying the photophysics of photo-induced proton transfer processes in general [1] and excited state intramolecular proton transfer (ESIPT) in particular [2, 3]. The latter process involves intramolecular hydrogen bond interactions (between the acidic and basic centers) in the S_0 state and the charge

Electronic supplementary material The online version of this article (doi:10.1007/s10953-010-9639-1) contains supplementary material, which is available to authorized users.

J. Premakumari · G.A.G. Roy
Department of Chemistry, Scott Christian College, Nagercoil 629 002, India

A.A.M. Prabhu · G. Venkatesh · V.K. Subramanian · N. Rajendiran (✉)
Department of Chemistry, Annamalai University, Annamalai Nagar 608 002, Tamilnadu, India
e-mail: drrajendiran@rediffmail.com

density distribution changes upon excitation of these molecules to their first excited singlet state (S_1). These changes in the acidic and basic properties of the aromatic systems are due to difference in the charge distribution upon excitation to S_1 and thus may also change the photophysics of the molecules. This induces large changes in their acidic and basic properties and thus leads to proton transfer along the hydrogen bond in a tautomerization process. ESIPT is generally very fast and takes place almost without activation energy. A number of molecules showing ESIPT behavior have been investigated thoroughly and these molecules have been used in dye lasers, polymer photo-stabilizers [4], high energy radiation detectors [5], molecular energy storage [6] and as fluorescent probes [7]. It has been observed that the acidic and basic characteristics of these kinds of molecules are very different from one another.

In addition to the solvent data, studies of the inclusion complexation of organic molecules with cyclodextrins (CD) also provide some useful information about the geometry of guest molecules. A generally accepted reason for choosing CDs, a class of cyclic oligosaccharides with 6–8 D-glucose units linked by α-1,4-glucose bonds, as the starting materials to construct supramolecular architectures is that the truncated cone-shaped hydrophobic cavities of CDs have a remarkable ability to include various guest molecules, either in solution or in the solid state, to form the functional host-guest inclusion complexes [8, 9] which can be used subsequently as the building blocks of supramolecular aggregates. Among the various families of organic compounds used as guest molecules, chromophoric guests such as azobenzenes [10–16] are of particular importance because they can exhibit appreciable spectral changes upon inclusion within CDs in solution, and thus can be applied as versatile spectral probes to investigate host–guest complexation. However, comparative studies on the inclusion complexation behavior of CDs with azo derivatives are still rare, to the best of our knowledge, although azo derivatives are widely focused upon because of their potential to construct photodriven molecular machines [10]. In this regard, the present study describes the photophysics of 2,4-dihydroxyazobenzene (sudan orange-G, DHAB), 4-hydroxyazobenzene (HAB) and azobenzene (AB) in various solvents, pH and β-CD concentrations.

2 Experimental

2.1 Instruments

Absorption measurements were carried out with a Hitachi Model U-2001 UV-visible spectrophotometer and fluorescence measurements were made with a Shimadzu RF 5301 spectrofluorometer. The pH values, in the range 2.0–12.0, were measured using an Elico pH meter model LI-120. FT-IR spectra were obtained using an Avatar-330 FT-IR spectrometer in the range 500–4000 cm^{-1} using KBr pelleting. Microscopic morphological structure measurements were made with a JEOL JSM 5610LV scanning electron microscope. A Bruker Advance DRX 400 MHz super conducting NMR spectrophotometer was used to record ^1H NMR spectra.

2.2 Reagents and Materials

DHAB, HAB, AB, β-CD and spectrograde solvents were obtained from the Sigma-Aldrich chemical company and used as such. The purity of the compound was checked by similar fluorescence spectra when excited with different excitation wavelengths. Triply distilled water was used for the preparation of aqueous solutions. Solutions in the pH range 2.0–12.0

Table 1 Absorption, fluorescence spectral data (nm) and Stokes shifts (cm^{-1}) of DHAB, HAB and AB in selected solvents

No.	Solvents	DHAB				HAB				AB			
		λ_{abs}	$\log_{10}\varepsilon$	λ_{flu}	Stokes shift	λ_{abs}	$\log_{10}\varepsilon$	λ_{flu}	Stokes shift	λ_{abs}	$\log_{10}\varepsilon$	λ_{flu}	Stokes shift
1	Cyclohexane	382	4.32	422	3030	340	4.27	380	2745	313	4.25	370	4922
		258	3.81			235	3.90			228	3.85		
2	Dioxane	380	4.32	430	3059	345	4.34	385	3012	319	4.21	361	3647
		255	3.78			237	3.97			229	3.89		
3	Acetonitrile	380	4.22	430	3059	345	4.31	390	3079	316	4.35	360	3868
		257	3.84			237	3.97			227	3.86		
4	2-Propanol	382	4.45	432	3030	345	4.23	390	3079	316	4.31	362	4022
		259	3.85			235	3.82			226	3.92		
5	Methanol	381	4.46	432	3099	345	4.28	395	3079	316	4.33	362	4022
		258	3.87			235	3.89			227	3.94		
6	Water	375	4.53	430	3411	342	4.23	400	3333	324	4.32	366	3542
		254	3.98			228	3.84			228	3.94		
7	Correlation coefficient												
	$\Delta\overline{\nu}_{ss}$ versus $E_T(30)$			0.9229				0.9181				0.9013	
8	$\Delta\overline{\nu}_{ss}$ versus BK			0.7593				0.7196				0.7236	

were prepared with appropriate amounts of NaOH and H_3PO_4. A modified Hammett's acidity scale (H_0) [17] for the solutions below pH $\sim$ 2 (using H_2SO_4–H_2O mixtures) and Yagil's basicity scale (H_) [18] for solutions above pH$\sim$ 12 (using NaOH–H_2O mixtures) were employed. The solutions were prepared just before each measurement. The concentration of the DHAB, HAB and AB solutions was of the order of 2×10^{-4} to 2×10^{-5} mol·dm^{-3} and that of β-CD the solution was varied from 1×10^{-3} to 1×10^{-2} mol·dm^{-3}. The solid inclusion complex was prepared by co-precipitation.

3 Results and Discussion

3.1 Effect of Solvents

The absorption maxima, emission maxima, molar extinction coefficient and Stokes shifts of DHAB, HAB and AB were studied in different solvents (Table 1). Similar to that of AB, the absorption bands of both hydroxyazobenzenes consisted of two peaks in all the solvents. The AB longer wavelength band (LW) shows a small red shift from non-polar to polar solvents, whereas a large red shift was noticed in the shorter wavelength band (SW). Unlike AB, the absorption maximum of DHAB/HAB is blue shifted in water. When compared to AB the LW band in DHAB and HAB are more red shifted than the SW and (cyclohexane, LW $\approx$ 67 nm, SW $\approx$ 10 nm in DHAB and LW $\approx$ 27 nm, SW $\approx$ 10 nm in HAB). The data in Table 1 reveal that the positions of both bands are not influenced by changing the solvent. Though there is no discernible effect (not more than a few nanometers) of solvent polarity on the absorption maxima, the observed spectral shifts in the absorption spectra of the DHAB/HAB in aprotic and protic solvents are consistent with the characteristic behavior of the hydroxyl group [19–26].

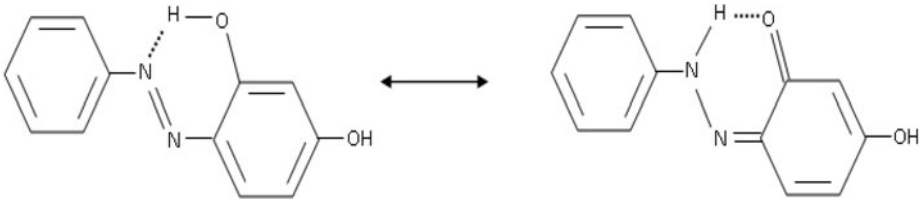

Fig. 1 Intramolecular hydrogen bonding structure in DHAB

The absorption maxima of DHAB (cyclohexane: $\lambda_{abs} \sim 382, 256$ nm, $\lambda_{flu} \sim 422$ nm) is red shifted more than that of HAB (cyclohexane: $\lambda_{abs} \sim 340, 235$ nm, $\lambda_{flu} \sim 380$ nm) and AB (cyclohexane: $\lambda_{abs} \sim 313, 228$ nm, $\lambda_{flu} \sim 370$ nm) in all solvents. For DHAB, the absorption maxima at 382, 256 nm in a non-polar solvent suggests the presence of intramolecular hydrogen bonding interaction (IHB) between –OH···N=N– groups (Fig. 1). The molar extinction coefficient is very high ($\sim 10^{-4}$ cm^{-1}) and the absorption maximum is slightly blue shifted in water from 382 nm to 375 nm, which implies that the IHB band is affected by the polar solvents.

In all the solvents, the fluorescence spectra of DHAB, HAB and AB molecules show a single emission. The emission spectra of DHAB, HAB and AB are excited at 370 nm, 340 nm and 320 nm respectively. In DHAB, the emission maximum appears at around 422–430 nm, whereas for HAB it is seen at around 380–400 nm and for AB it is seen at 370 nm. In any one solvent, when compared to 4-aminoazobenzene [26] (AAB, cyclohexane: $\lambda_{abs} \sim 370, 246$ nm, $\lambda_{flu} \sim 425$ nm), the absorption and emission spectra of HAB give blue shifted maxima whereas the DHAB molecule gives red shifted maxima. The above results reveal that the absorption and fluorescence spectral shifts of the hydroxyl group on the aromatic ring is less than that of amino group both in the ground and excited singlet states. However, in DHAB because of IHB, the absorption and fluorescence maxima are more red shifted than those of AAB and HAB molecules (Table 1).

In contrast to azonaphthol, the azophenol compounds (DHAB, HAB) do not exist as tautomer mixtures in solution at room temperature, e.g., azonaphthol molecules are present in both azo (A) and hydrazo form (H) and their relative stability depends on the solvent and/or temperature [27–30]. The tautomeric behavior of azonaphthol compounds differs considerably from that of the corresponding azophenols [27] which exist mainly in the azo form at room temperature, even in polar solvents. Such a difference may be caused by the loss of aromaticity on going from the azo to hydrazo form, while for the azonaphthol compounds this effect is compensated by the transfer of aromaticity within the naphthalene fragment; i.e. in azophenols, the number of localized electrons in the tautomeric phenyl ring is reduced from six to four in the hydrazo form. This is because two of these electrons are engaged in strong C=N and C=O bonds and thus, the phenyl ring looses much of its aromaticity. In the naphthalene compounds, this effect is compensated by the second aromatic ring [30]. Therefore, the emission maximum appears around 430 nm because only the azo form exists for both of the molecules.

3.2 Correlation of Solvatochromic Shift with the Solvent Polarity

When a solute is placed in a solvent, the combined effects of general and specific interactions are observed and the separation of these interactions is often difficult. Empirically or theoretically derived solvent parameters like the Biolet-Kawaski (*BK*) [31] and Reichardt and Dimroth's, $E_T(30)$ [32] values, as accurate registers of solvent polarity, have been used to

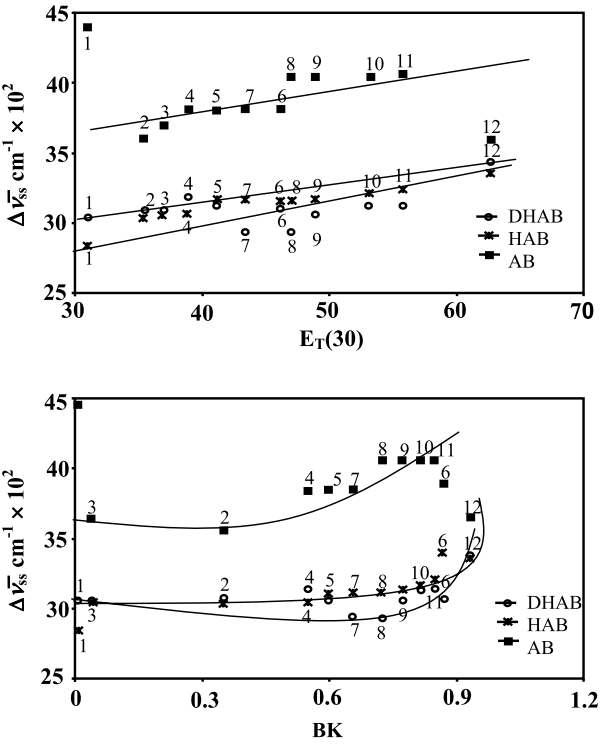

Fig. 2 Plot of Stokes shifts (cm^{-1}) of DHAB, HAB and AB versus $E_T(30)$ and *BK* solvent parameters: (1) cyclohexane, (2) diethyl ether, (3) 1,4-dioxane, (4) ethylacetate, (5) dichloromethane, (6) acetonitrile, (7) *t*-butyl alcohol, (8) 2-butanol, (9) 2-propanol, (10) ethanol, (11) methanol, (12) water

correlate molecular spectroscopic properties (Table 1). Among these parameters, *BK* takes into account the solvent polarity alone, whereas the $E_T(30)$ solvent polarity parameter is based on the spectral shifts of *N*-phenol betaine in different solvents of varying polarity and hydrogen bonding effects. Correlation of the Stokes shifts with any one of these parameters gives an idea about the type of interaction between the solute and solvent. A very good linearity is found in the plot of Stokes shifts *versus* $E_T(30)$.

The large red shift of DHAB, HAB and AB molecules in protic solvents may be the result of hydrogen bond formation between specific sites of the solute and solvent molecules. A good correlation of the Stokes shifts with the $E_T(30)$ scale indicates hydrogen bonding interaction is predominant and the dipole moment difference between the excited state and the ground state is large. Figure 2 shows a dramatic change in slope at the intermediate polarity region; thus, the plots are non-linear. The large deviations in hydroxylic solvents can be explained as follows. It is well established that the –OH group becomes more acidic in the S_1 state and can donate a proton easily to the solvent. In contrast in the S_0 state the –OH group acts as a proton acceptor. This means that the hydrogen bond between the solvent molecule and the lone pair of the –OH group in the S_0 state is broken on excitation and a hydrogen bond is formed between the proton of the –OH group and the lone pair of the solvent molecule. As a result, in polar and non-polar solvents, a non-linear plot is observed for azo molecules.

3.3 Effect of pH

The effect of proton concentration on the absorption and fluorescence spectra of DHAB and HAB is different to that observed for other aromatic hydroxyl compounds [29, 30]. The

Table 2 Various prototropic maxima (absorption and fluorescence) of DHAB, HAB and AB in aqueous and β-CD medium

Species	DHAB				HAB				AB			
	Aqueous medium		β-CD medium		Aqueous medium		β-CD medium		Aqueous medium		β-CD medium	
	λ_{abs}	λ_{flu}	λ_{abs}	λ_{flu}	λ_{abs}	λ_{flu}	λ_{abs}	λ_{flu}	λ_{abs}	λ_{flu}	λ_{abs}	λ_{flu}
Dication	426	430			426	430						
Mono-	458	485	458	490	457	488	456	492	420	425		
cation	251		251		232		234		250			
	218		218									
Neutral	375	430	379	455	342	388	342	454	318	370	320	370
	254		256		230		234		228		223	
	219		220s									
Mono-	430	510	420	490	430	498	420	490				
anion	248	410	300		260			389				
	217	333	230									
Dianion	480	520w										
	403s	430										
	263											

q—quenching, w—weakly fluorescent

absorption and fluorescence spectra of various prototropic species are shown in Table 2. The protonation spectral shifts of DHAB and HAB molecules follow a similar trend in acid and base environments. In both S_0 and S_1 states, with an increase of pH from 4 to 8, the absorption and emission spectra move to longer wavelengths in DHAB/HAB showing that deprotonation takes place at the hydroxyl group (i.e. a monoanion is formed). In DHAB, when the basicity is increased above pH ~ 8 the absorption and emission spectra are again shifted to longer wavelengths ($\lambda_{abs} \sim 480, 263$ nm, $\lambda_{flu} \sim 520$ nm) suggesting formation of a dianion. In azo molecules, the large red shifted absorption and emission spectra observed in monoanion and dianion species indicate the presence of a greater degree of interaction between the aromatic rings.

With decreases of pH from 2.5 to $H_0 - 1$, large red shifted absorption and emission maxima are observed in the S_0 and S_1 states indicating that protonation takes place at the azo group. Further, a regular red shift suggests azo-hydrazo tautomer formation occurs in both molecules. This assumption is based on the following: it is well known that, if protonation takes place at the amino or hydroxyl group, (i) a blue shifted spectrum should be observed, and (ii) the absorption maximum should resemble that of the parent AB molecule. This is because the protonation will block the amino or hydroxyl group lone pair electrons and thus the absorption spectrum should resemble that of the parent AB molecule.

The protonation behavior of HAB in dilute acid has been examined previously [33–36]. In 20% aqueous sulphuric acid, Klotz et al. [34] reported a pK_a value of -0.93 (monocation–neutral) and in aqueous sulphuric acid containing 20% ethanol, a pK_a of ~ 1.02 has been observed by Yeh and Jaffe [33]. These data were confirmed by Strachan et al. [35] by using 5% dioxane and 95% aqueous H_2SO_4 medium. For the neutral form of DHAB and HAB, λ_{max} were found to be 375 nm and 342 nm, respectively, and for the protonated form of both molecules λ_{max} was 457 nm, with pK_a -0.99 in the aqueous medium.

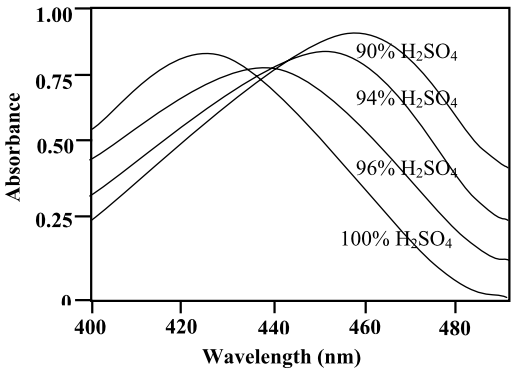

Fig. 3 Absorption spectra of HAB in various concentrations of H_2SO_4

Above 50% H_2SO_4 (corresponding to about 99% protonation) no significant changes were observed in λ_{max} until about 90% H_2SO_4, and the spectral absorption was also time invariant.

In 90–100% H_2SO_4, both DHAB and HAB molecules have been observed to undergo further spectral changes which are time dependent. In the region ∼90% H_2SO_4 the initial λ_{max} is unchanged at 457 nm, but with time this absorbance increases and is simultaneously shifted to 465 nm (Fig. 6). In the 100% H_2SO_4 region, the initial absorption gradually shifts to shorter wavelengths until it reaches to 426 nm (Fig. 3). In these acidities the growth in peak height is more rapid and the product spectra exhibit a concurrent gradual shift to 450 nm. The above time dependent spectral changes were shown to be the result of the conversion of 4-hydroxyazobenzene to the 4-hydroxyazobenzene–4′-sulphonic acid [35]. Initial HAB spectra obtained for the 90–100% H_2SO_4 region over 460 nm are shown in Fig. 6. The immediate spectral shifts are due to protolytic equilibrium. These have the general character that results from a protonation process in which medium effects may be responsible for the poorly defined isosbestic point [36]. Therefore, the 426 nm absorption is ascribed to diprotonated form of DHAB and HAB.

In order to obtain pK_a values for all of the corresponding equilibria (i.e., dication–monocation, monocation–neutral, neutral–monoanion, monoanion–dianion), when the absorbance and emission intensity data plotted against H_0/pH/H_- a typical sigmoid curve is obtained. From the inflexion point, the pK_a (dication–monocation) value of –10.1 is obtained for DHAB as a first approximation. Application of the convergence method of Arnett and Wu [37] to these data yields a pK_a ∼10.2 (Table 3).

The protonation behavior of 4-hydroxyazobenzene–4′-sulphonic acid in dilute acidic conditions has been already reported by Reeves [38]. The pK_a (monocation–neutral) for protonation of the azo group was reported as −1.45, λ_B is 350 nm and λ_{BH}^{+} is 464 nm in aqueous medium. In the present work, the spectral of the DHAB compound was analyzed and compared to HAB in the acid and base regions. The spectra were stable except in very high acid concentrations and slow changes were observed which can be ascribed to a second sulphonation process. Some of the spectra are reproduced in Fig. 6 and are seen to exhibit reasonably good isosbestic point behavior. For the determination of pK_a (dication-monocation), absorbance data were measured at 455 nm and at 426 nm as a function of acid concentration. The neutral-monoanion equilibrium in the S_0 and S_1 states also yields a sigmoid curve. The plot of the extinction as a function of H_0 gave a typical sigmoid curve, from which a visual value of pK_a −11.0 is obtained.

The basic center in the first protonation of HAB and related compounds are generally [39] taken to be the β-nitrogen, in accord with resonance stabilization of charge at that

Table 3 The ground and excited state acidity constant (pK_a and pK_a^*)[a] values of different prototropic equilibria of DHAB, HAB and AB in the S_0 and S_1 states

Equilibrium	DHAB				HAB				AB			
	Aqueous medium		β-CD medium		Aqueous medium		β-CD medium		Aqueous medium		β-CD medium	
	pK_a abs	pK_a^* FT	pK_a abs	pK_a^* FT	pK_a abs	pK_a^* FT	pK_a abs	pK_a^* FT	pK_a abs	pK_a^* FT	pK_a abs	pK_a^* FT
Monocation	0.81	0.62	0.76	0.62	−0.85	0.92	0.74	0.82	−2.48	−2.50		
Neutral												
Neutral												
Monoanion	6.5	6.8	6.6	6.9	6.6	6.8	6.7	6.9				
Monoanion												
Dianion	12.2	13.6										

[a]The uncertainties in pK_a and pK_a^* are ±0.2

Fig. 4 Monocation resonance stabilization structure in HAB

Fig. 5 Second equilibrium protonation in the aromatic carbon and phenolic oxygen in HAB

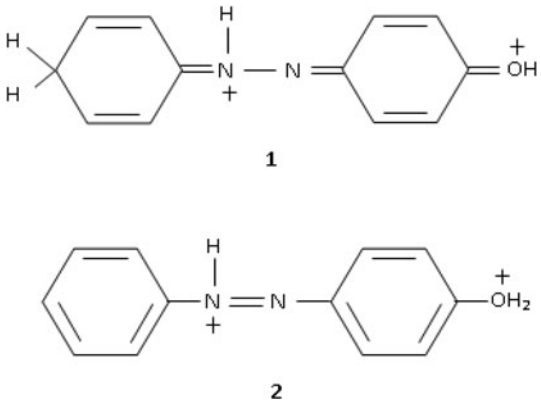

position (Fig. 4). The second protonation equilibrium, which is observed in concentrated acid media, may occur on an aromatic carbon to give a delocalized structure such as 1, or on the phenolic oxygen in which case the localized structure 2 results (Fig. 5).

Aromatic ring protonation of alkyl benzenes such as mesitylene in HF-BF_3 [40] or HSO_3F [41] is well established. Carbon protonation is also observed with phloroglucinol (and its alkyl ethers) in fluorosulphonic acid or aqueous perchloric acid [42]. The site of protonation in these instances is deduced from nuclear magnetic resonance data. These processes are also characterized by the appearance of a new peak at 350 nm in the absorption spectrum. For phenol, anisole, and the dialkoxy analogues the protonation process

Fig. 6 Diprotonated species in the HAB molecule

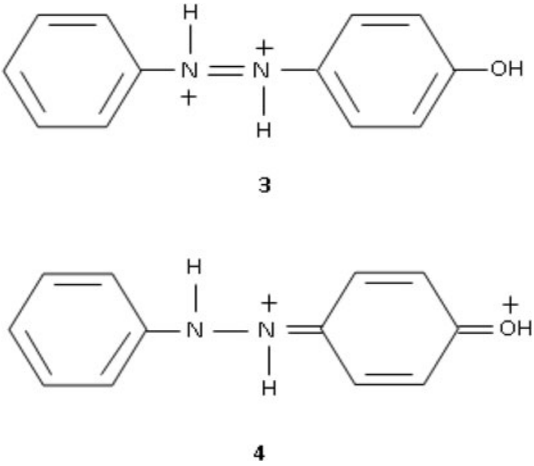

in aqueous acid is less clear and both O- and C-protonation have been suggested to occur by different workers [43, 44].

If the second protonation of HAB had occurred on a carbon (Fig. 5 structure 1) then the π-electron distribution should have been perturbed considerably and one would have expected a spectral shift in the UV-visible region to longer wavelength, by analogy with the other aromatic compounds discussed above. On the other hand, protonation of the phenolic oxygen, by the removal of the π-electrons of oxygen from the aromatic resonance system should result in a dicationic species (2) which is iso π-electronic with the protonated azobenzene cation. The absorbance of the latter (424 nm) is in fact very close to the absorption of the observed for the diprotonated species (426 nm). This is taken as evidence that the second conjugate acid of HAB has structure 2.

The possibility that the second protonation occurs on the azo group, to give structure 3, may also be considered (Fig. 6). However in that case, structure 4 should be an important contributor, by analogy with monoprotonated DHAB/HAB. Consequently one would expect diprotonated DHAB/HAB to have its absorption maximum largely unchanged from the monoprotonated form, which is not the case. A noteworthy point is that azobenzene itself apparently does not undergo a second protonation even in 100% H_2SO_4, which suggests that protonation of both nitrogen in the azo group is relatively unfavorable.

3.4 Effect of β-CD

Table 4 and Fig. 7 depict the recorded absorption spectra of DHAB, HAB and AB in aqueous solution containing different concentrations of β-CD. The absorption spectrum of DHAB/HAB molecules (DHAB, $\lambda_{abs} \sim 380, 256$ nm, HAB, $\lambda_{abs} \sim 340$ nm) shows a slight blue shift whereas no significant shift is observed in AB ($\lambda_{abs} \sim 319$ nm). In AB molecule, a slight increase in the molar extinction coefficient occurs with increasing β-CD concentration from 1×10^{-3} M to 1×10^{-2} M. The absorbance of the solutions recorded after 12 hours remains constant indicating that the molecules are present in the β-CD cavity in solution without decomposing on storage due to formation of inclusion complex. The measured absorbance, plotted against the solution concentration [β-CD] is shown in the insert of Fig. 8. The absorbance increases in DHAB, HAB and AB indicate the encapsulation of these molecules in the β-CD cavity and it is attributed to the detergent action of β-CD. A clear

Table 4 Absorption and fluorescence maxima (nm) of DHAB, HAB and AB in different β-CD concentrations

Concentration of β-CD ($mol \cdot dm^{-3}$)	DHAB			HAB			AB		
	λ_{abs}	$\log_{10} \varepsilon$	λ_{flu}	λ_{abs}	$\log_{10} \varepsilon$	λ_{flu}	λ_{abs}	$\log_{10} \varepsilon$	λ_{flu}
Water	382	4.53	430	342	3.96	390	319	4.25	370
	249	3.98		228	3.77		228	3.90	
	220s	4.10							
0.001	380	4.27	455	340	3.98	452	319	4.30	370
	256	4.03		229	3.86		230	3.95	
	220s	4.15							
0.002	379	4.29	457	340	3.99	452	320	4.35	370
	256	4.10		230	3.66		232	3.97	
	220s	4.17							
0.004	379	4.30	458	340	4.00	452	320	4.42	370
	256	4.22		238	3.68		233	4.13	
	220s	4.25							
0.006	379	4.31	460	340	4.01	452	320	4.47	370
	256	4.33		239	3.86		233	4.24	
	220s	4.35							
0.008	379	4.31	460	340	4.01	451	320	4.50	370
	256	4.42		240	3.86		233	4.35	
0.010	379	4.39	460	340	4.02	451	320	4.51	370
	256	4.50		240	3.86		233	4.43	
Excitation wavelength	360			340			290		
Binding constant ($dm^3 \cdot mol^{-1}$)	945		1155	550		636	475		548
ΔG ($kJ \cdot mol^{-1}$)	−17.75		−17.96	−15.88		−16.27	−15.53		−15.87

isosbestic point is observed in the absorption spectra indicating that a simple 1:1 inclusion equilibrium exists.

Figure 8 shows the fluorescence spectra of DHAB, HAB and AB in different concentrations of β-CD. In β-CD solutions, the fluorescence spectra of the above molecules are more sensitive than the absorption spectra. As the β-CD concentration is increased, the fluorescence intensity of AB molecule increases significantly at the same emission wavelength (370 nm). The emission maxima of both hydroxyl compounds are largely red shifted from 390–410 nm to ∼458 nm and the emission intensities increase with increasing β-CD concentrations. Such a change in the emission maxima of both molecules caused by the introduction of β-CD indicates the formation of an inclusion complex. The considerable increase in the fluorescence intensity compared with absorbance shows that the quantum yields of both molecules increase in the presence of β-CD.

In general, the existence of an isosbestic point in the absorption spectra is an indication of the formation of a well defined 1:1 inclusion complex [19–27, 45, 46]. For a 1:1 complex between β-CD and a guest molecule (DHAB, HAB and AB), the following equilibrium can

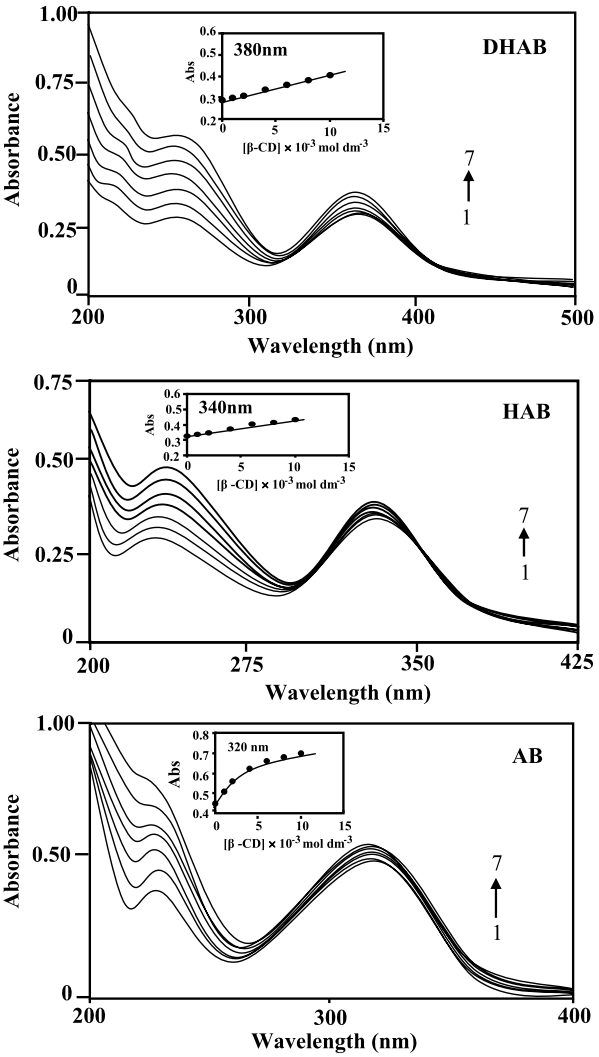

Fig. 7 Absorbance spectra of DHAB, HAB and AB in different β-CD concentrations (mol·dm^{-3}): (1) 0, (2) 0.001, (3) 0.002, (4) 0.004, (5) 0.006, (6) 0.008, and (7) 0.01

be written:

$$\mathrm{DHAB} + \beta\text{-CD} \rightleftharpoons \mathrm{DHAB}\cdots\beta\text{-CD} \tag{1}$$

The formation constant K and stoichiometric ratios of the inclusion complex of DHAB/HAB can be determined according to the Benesi–Hildebrand [47] relationship assuming the formation of a 1:1 host–guest complex (Eq. 2):

$$\frac{1}{\Delta A} = \frac{1}{\Delta\varepsilon} + \frac{1}{K[\mathrm{DHAB}]_0\Delta\varepsilon[\beta\text{-CD}]_0} \tag{2}$$

where ΔA is the difference between the absorbance of DHAB/HAB in the presence and absence of β-CD, $\Delta\varepsilon$ is the difference between the molar absorption coefficients of DHAB/HAB and the inclusion complex, and $[\mathrm{DHAB}]_0$ and $[\beta\text{-CD}]_0$ are the initial concentrations of DHAB/HAB and β-CD, respectively. A good linear correlation is obtained

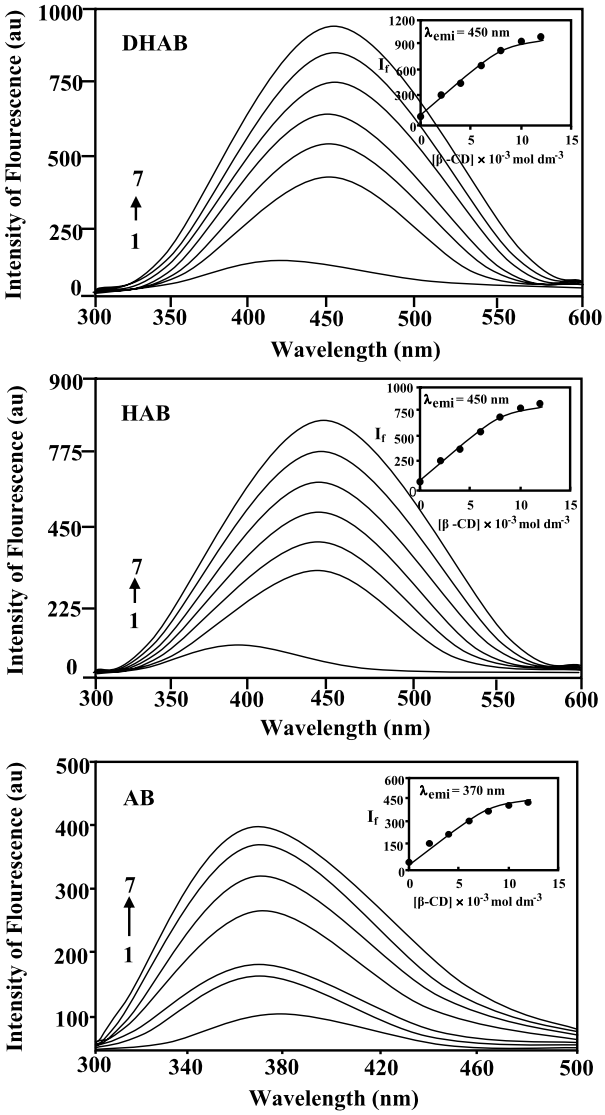

Fig. 8 Fluorescence spectra of DHAB, HAB and AB in different β-CD concentrations (mol·dm^{-3}): (1) 0, (2) 0.001, (3) 0.002, (4) 0.004, (5) 0.006, (6) 0.008, and (7) 0.01

between a plot of $1/\Delta A$ and $1/[\beta\text{-CD}]$ (Fig. 9) confirming the formation of a 2:2 inclusion complex. The value of the association constant K for the inclusion complexation is obtained from the slope and intercept of the above plot.

The dependence of concentration of β-CD on fluorescence was also analyzed by the Benesi–Hildebrand [47] plot as given by Eq. 3:

$$\frac{1}{I - I_0} = \frac{1}{I' - I_0} + \frac{1}{K(I' - I_0)[\beta\text{-CD}]_0} \tag{3}$$

where $[\beta\text{-CD}]_0$ represents the initial concentration of β-CD, I_0 and I are the fluorescence intensities in the absence and presence of β-CD respectively. According to Eq. 3 a plot of

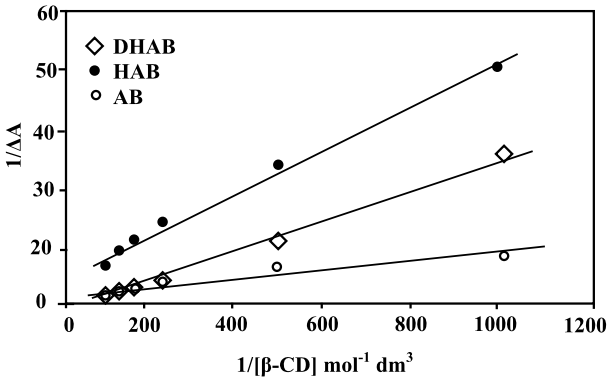

Fig. 9 Absorption spectra Benesi-Hildebrand plot for the complexation of DHAB, HAB and AB with β-CD (plot of $1/\Delta A$ versus $1/[\beta\text{-CD}]$)

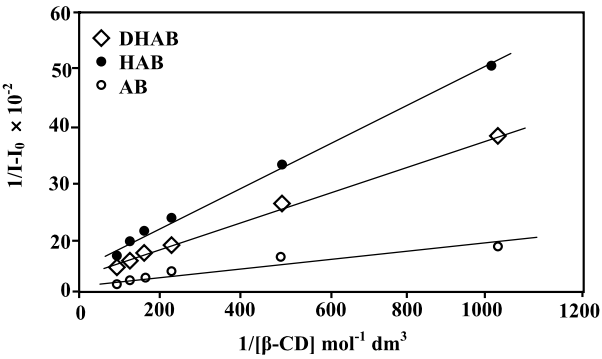

Fig. 10 Fluorescence spectra Benesi-Hildebrand plot for the complexation of DHAB, HAB and AB with β-CD (plot of $1/I - I_0$ versus $1/[\beta\text{-CD}]$)

$1/(I - I_0)$ versus $1/[\beta\text{-CD}]$ also shows excellent linear regression further supporting the formation of a 2:2 inclusion complex (Fig. 10).

The Gibbs energy change of this complex can be calculated from the following equation

$$\Delta G = -RT \ln K \tag{4}$$

As can be seen from Table 4, the negative ΔG values suggest that the inclusion process proceeds simultaneously at 303 K. The negative values under the experimental conditions indicate that the inclusion process is an exothermic and enthalpy controlled process. The negative enthalpy change arose from the van der Waals interaction caused by molecular geometry and the limitations of the β-CD cavity.

Many researchers has demonstrated that host:guest (size/shape) matching and hydrogen bond interactions can lead to stronger van der Waals and hydrophobic interactions [48] and this may enhance the binding between guest molecules with β-CD. These interactions are mainly dependent on the host–guest distance and contact surface area [48]. The binding constant for the inclusion complexation of DHAB with β-CD, 945 $dm^3 \cdot mol^{-1}$, is higher than that of the HAB:β-CD complex (550 $dm^3 \cdot mol^{-1}$). The formation constant of HAB is small compared to that of the DHAB molecule. This is probably because the HAB molecule is not tightly encapsulated in the β-CD cavity, whereas in DHAB the presence of an *ortho* hydroxyl group might have enabled encapsulation and increased the formation constant. The higher binding constant of DHAB may be attributed to its size/shape fit within the host β-CD cavity. Further, the included DHAB molecule enhances the IHB interactions because the

IHB ring of DHAB is tightly encapsulated in the β-CD cavity. The IHB interactions result in strong van der Waals and hydrophobic interactions between the guest and host. Owing to these strengthened guest host interactions, the DHAB inclusion complex has a higher binding constant value than that of HAB.

3.5 Possible Inclusion Complex

From the models suggested by Liu et al. [49] on β-CD–HAB inclusion complexes, we can deduce that the azobenzene moiety of DHAB/HAB is included longitudinally in the β-CD cavity. The emission spectrum of DHAB/HAB in aqueous β-CD solutions shows a longer wavelength emission around 455 nm which is assigned to a higher conjugated system occurring between two benzene rings; i.e., the two benzene rings are almost located in the same plane. Further, our studies on the other azo compounds 4-aminoazobenzene and 4-amino-2′,3-dimethyl azobenzene molecules [26] also exhibit an emission maximum at 455 nm similar to DHAB, HAB suggesting that both benzene rings are located in the same manner. In DHAB/HAB, the emission intensity is greatly enhanced with the red shift, whereas in AB the emission intensity is enhanced at the same wavelength, which implies that the inclusion processes for the DHAB/HAB molecules are different from that for the AB molecule.

In DHAB/HAB, a large bathochromic shift along with an increase in the fluorescence intensity in β-CD solutions (400 to 455 nm), as compared to that in aqueous solution, is explained as follows: both molecules are embedded in two β-CD cavities in different directions to form the head-to-head dimer arrangement while the –OH group of both molecules points to the primary side of the β-CD cavity [48]. This unusual dimerization behavior is attributed to the cooperative interactions of eight hydrogen bonds between the secondary hydroxyl groups of two adjacent β-CD units as well as the π–π^* interaction between the benzene rings. Two guest molecules are embedded into two β-CD cavities in two different directions with the –OH group of the azo molecules pointing towards the primary side of the β-CD cavity, i.e. 2:2 stoichiometry between DHAB and HAB with β-CD occurs (Fig. 11). Moreover, two β-CD–DHAB or β-CD–HAB complexes are connected by hydrogen bonds from the hydroxyl groups of the two benzene rings in a head-to-head fashion to form a dimer unit.

More interestingly, two adjacent head-to-head β-CD–DHAB or β-CD–HAB dimers adopt different orientations, which consequently result in the formation of longer wavelength emission maxima. Further, water molecules are located on the exterior part of the β-CD cavities and both benzene rings are included in the β-CD cavity, which indicates the presence of strong hydrophobic interactions between the guests and β-CD cavities. On the other hand, the strong H-bond network formed by the –OH groups of β-CD and the –OH group of azobenzene further enhance the longer wavelength emission. In the β-CD/HAB dimer, two hydroxyl groups of the HAB molecule participate in the formation of the inter dimer H-bonds leading to the bathochromic shift.

Let us now consider other possible types of inclusion complexes: (i) if the azo molecule is partially (i.e. the benzene ring) entrapped in to the β-CD cavity, like in the AB molecule in β-CD solutions, and if this type of inclusion complex is formed, then the fluorescence intensity of DHAB/HAB should increase at the same wavelength in the β-CD solutions and, (ii) if another part of azo molecule (i.e., the –OH group attached to the phenyl ring) is encapsulated in the β-CD cavity, then the monoanion absorption and emission maxima (i.e., deprotonation of hydroxyl group) should be blue shifted in β-CD as compared to the aqueous medium.

To know the effect of β-CD on the prototropic equilibrium between neutral, monocation and monoanion, the pH dependent changes in the absorption and emission spectra of both

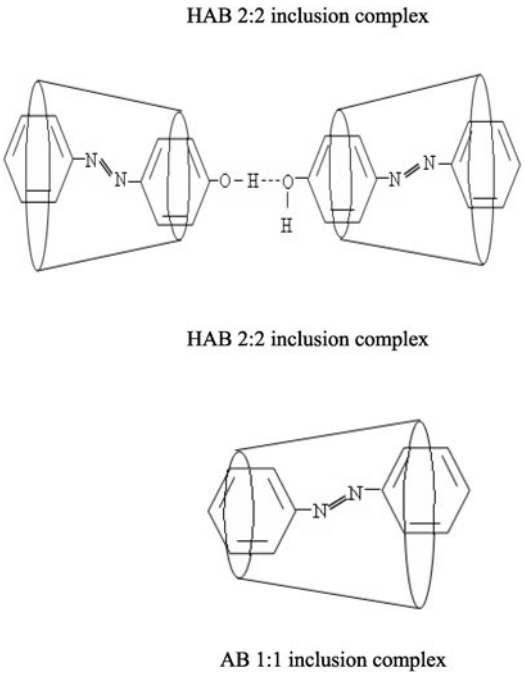

Fig. 11 Proposed inclusion complex structure of DHAB, HAB and AB

molecules in aqueous solution containing β-CD have been recorded and are shown in Table 2. The absorption and emission maxima have been studied in 6×10^{-3} mol·dm^{-3} β-CD solutions in the pH range 0.1 to 11. When compared to the aqueous medium, the absorption maxima of both molecules are slightly blue shifted in the β-CD medium whereas the emission maxima are largely red shifted as compared to the aqueous medium and the monoanion maxima are slightly blue shifted in the β-CD medium.

The tendencies of these shifts in λ_{abs} and λ_{flu} are attributable to the inclusion of both molecules in the β-CD cavity. The ground and excited state pK_a (pK_a^*) values of HAB molecules in the β-CD medium are slightly different as compared to the aqueous medium (Table 3). This is because the formation of a guest–β-CD complex i.e., in the inclusion complex pK_a (pK_a^*) values are known to change depending upon the relative affinity of the guest and host.

The results in Table 4 indicate that the neutral maxima of DHAB/HAB in β-CD are largely red shifted as compared to aqueous medium and the monoanion maxima are slightly blue shifted in the β-CD medium. It has been reported that when the $-$OH group is entrapped in the β-CD cavity, the monoanion maxima should be largely blue shifted in β-CD medium as compared to the aqueous medium [19–27, 45]. This suggests that the environment around the OH group in the β-CD medium is same as in the bulk aqueous medium. Since the viscosity is increased in the β-CD solutions, a slight blue shift is observed in the monoanion maxima.

Semi-empirical quantum chemical calculations also provide some useful information about the inclusion complexation geometry of guest molecules. To determine the dimensions of DHAB, HAB, and AB, geometries of these molecules and β-CD in the ground state were optimized by using the DFT level in the CAChe program [53–55]. This method provides acceptable approximations, which are quite close to the experimental findings. The internal diameter of the β-CD was found to be approximately 6.65 Å and its height ~7.8 Å

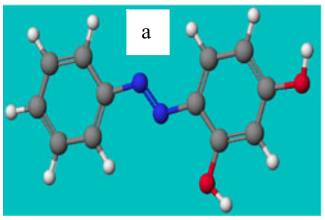

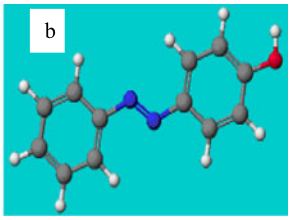

DHAB= ΔH = 10.1331 kcal/mol

H_3-H'$_3$= 11.98	C_4-C'$_4$= 9.21
H_3-H'$_4$= 10.93	C_4-H'$_3$= 10.30
H_6-H'$_5$= 5.32	O_2-C'$_4$= 10.58
H_1-H'$_4$= 5.65	O_2-H'$_4$= 11.67
H_8-N_1= 6.10	H_3-N_2= 6.64

HAB= ΔH = 55.2113 kcal/mol

H_3-H'$_4$= 12.55	H_3-C'$_3$= 10.11
H_3-H'$_2$= 10.89	H_3-C'$_2$= 8.805
H_3-C'$_4$=10.63	C_4-C'$_6$= 9.55
O_1-H'$_4$= 5.27	C_4-C'$_5$= 9.05

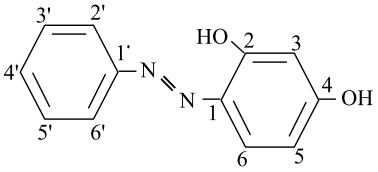

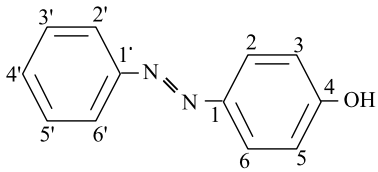

Fig. 12 DFT—CAChe (7.5 version) structure; (**a**) DHAB and (**b**) HAB

(Figs. 11 and 12). Considering the shape and dimensions of β-CD (Fig. 12), the above azo molecules cannot be completely encapsulated within the β-CD cavity. In the DHAB molecule, the distance between $H_4-H'_4$ is 11.403 Å, $H_4-H'_6$ is 7.781 Å, $H_4-H'_4$ is 8.200 Å, $C_4-C'_4$ is 9.210 Å, $C_3-C'_3$ is 7.816 Å, $C_4-C'_3$ is 8.706 Å, $H_4-C'_4$ is 10.306 Å, $H_4-C'_3$ is 9.587 Å, $H_4-C'_2$ is 8.425 Å. These values are greater than the inside diameter of the β-CD (7.8 Å) cavity. This may be responsible for the formation of different types of inclusion complexes with β-CD.

4 Solid Inclusion Complex Studies

4.1 Microscopic Morphological Observation

The powdered forms of DHAB, β-CD and their inclusion complexes were investigated by scanning electron microscopy (Fig. 13). This picture clearly shows the difference between DHAB and the inclusion complex. As seen from the SEM images (i) β-CD is present in a marble form, (ii) DHAB is present in the coral form and (iii) the structures of the inclusion complexes are different from those of the pure compounds. Modification of these structures can be taken as a proof for the formation of a new inclusion complex. The different structures of pure DHAB and their inclusion complex again supported the presence of solid inclusion complex.

4.2 Infrared Spectral Studies

The inclusion process of DHAB and its inclusion complex were investigated by the FT-IR spectra. In the spectra the −OH stretching frequency at 3059 cm^{-1} was shifted in the

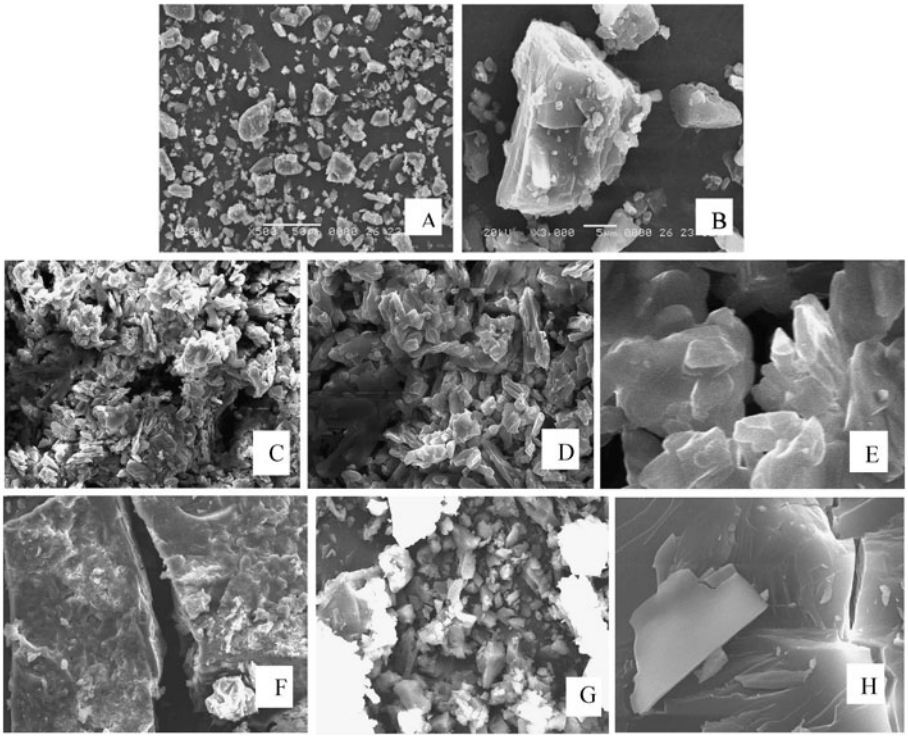

Fig. 13 SEM photographs (Pt. coated) β-CD = A (×500 μm), B (×3000 μm); pure DHAB = C(×500 μm), D (×1000 μm) and E (×5000 μm); inclusion complex of DHAB = F (×500 μm), G (×1000 μm) and H (×5000 μm)

inclusion complex to 3367 cm^{-1}. The aromatic ring stretching frequency at 1627 cm^{-1} and the aromatic C=C stretching frequency at 1590 cm^{-1} were shifted to 1622 cm^{-1} and 1618 cm^{-1}, respectively. The C–H bending vibrations at 857–682 cm^{-1} were shifted for the inclusion complex to 853–680 cm^{-1}. Further, the azo stretch at 1456 cm^{-1} was shifted in the inclusion complex to 1411 cm^{-1}. The above results indicate that (i) the DHAB molecule is encapsulated in the β-CD cavity, and (ii) the azo group is present inside the β-CD cavity. The above results confirmed that DHAB/HAB molecules are included in the β-CD cavity.

4.3 Proton Magnetic Resonance Spectral Studies

In order to comprehensively examine the structural features of the β-CD complexes and deeply understand the assembly process, the solution structures of DHAB, HAB and AB were investigated by means of NMR spectroscopy. Proton nuclear magnetic resonance (^{1}H NMR) spectroscopy has proved to be a powerful tool in the study of inclusion complexes [50–52]. ^{1}H NMR spectroscopy provides an effective means of assessing the dynamic interaction site of β-CD with guest molecules. The basis of information gained from NMR spectroscopy is located in these shifts, loss of resolution and broadening of signals observed for the host and guest protons [50–52]. The resonance assignments of the protons of β-CD are well established [50] and consist of six types of protons. The chemical shift of β-CD protons reported by different authors [50–52] are very close to those reported in this work.

Table 5 Chemical shifts (δ) of DHAB, HAB and AB and their inclusion complexes

Proton position	DHAB			HAB			AB		
	Pure	Complex	δ	Pure	Complex	δ	Pure	Complex	δ
^{2}H or (OH)	10.600	10.550	0.05	–	–	–	–	–	–
^{4}H or (OH)	12.500	12.522	−0.022	12.400	12.410	−0.010	–	–	–
^{3}H	6.328	6.338	−0.010	6.650	6.661	−0.011	7.495	7.503	−0.008
^{5}H	6.520	6.530	−0.010	6.650	6.661	−0.011	7.495	7.503	−0.008
^{6}H	7.701	7.661	0.040	7.750	7.741	0.009	7.920	7.912	0.008
$^{2'}$H, $^{6'}$H	7.860	7.857	0.003	7.690	7.660	0.030	7.920	7.911	0.009
$^{3'}$H, $^{5'}$H	7.552	7.549	0.003	7.440	7.420	0.020	7.495	7.484	0.009
$^{4'}$H	7.480	7.477	0.003	7.480	7.460	0.020	7.452	7.450	0.002

The H-3 and H-5 protons are located in the interior of the β-CDs cavity, and it is, therefore likely that the interaction of the host with β-CD inside the cavity affects the chemical shifts of the ^{3}H and ^{5}H protons. A minor shift is observed for the resonance of ^{1}H, ^{2}H and ^{4}H located on the exterior of β-CD [50].

Generally, the chemical shift values of the guest protons tend to show appreciable changes if the guest molecules are included in the β-CD cavities [50]. Therefore, H^1 NMR spectra of complexes of DHAB, HAB and AB were performed at 25 °C in D_2O and compared with those of pure compounds. As can be seen from Table 5, the δ-values of 3H, 5H are the protons of β-cyclodextrin, which shift down field and the δ-values of ^{2}H, ^{6}H, $^{2'}$H, $^{3'}$H, $^{4'}$H, $^{5'}$H and $^{6'}$H, protons shift up field as compared with the corresponding values for the free compounds. These results indicate that a host:guest inclusion complex is formed between DHAB, HAB, AB with β-CD in aqueous solution. Further, considering the structural features of the β-CD cavity, the ^{5}H and the ^{6}H protons located at the narrow side of the cavity and the ^{3}H protons near the wide side, we can deduce a possible inclusion geometry of inclusion complexes as given in Fig. 11.

As can be seen from the Table 5 the chemical shift data for the inclusion complexes are different from those of the free compounds. In particular, the resonance of the protons of β-CD located within or near the cavity showed a remarkable upfield shift (0.040 ppm) in the inclusion complex. In HABs, the aromatic ring hydrogens are downfield shifted in the complex, which suggested that the aromatic ring is largely shielded in the complex and it must penetrate deeply into the cavity. Further, as can be seen from Table 5, the resonances of DHAB/HAB protons within the β-CD cavity were shifted downfield when the inclusion complex was formed, which means that the DHAB/HAB has a preferred fixed orientation within the β-CD cavity.

5 Conclusion

The solvent studies show that only the azo form is only present in both the DHAB/HAB molecules. The unusually large red shifts observed in acidic solutions suggest that the azo-hydrazo tautomer is present in both molecules. In β-CD solutions, the increase in the fluorescence intensity and a large bathochromic shift in the S_1 state indicates that DHAB/HAB forms 2:2 inclusion complexes whereas AB forms a 1:1 inclusion complex. Head-to-head dimer are formed in both hydroxyl azobenzene compounds.

Acknowledgements This work was supported by the Department of Science and Technology, New Delhi (Fast Track Proposal Young Scientist Scheme No. SR/FTP/CS-14/2005) and University Grants Commission, New Delhi (Project No. F-31-98/2005 (SR). One of the authors Antony Muthu Prabhu is thankful to CSIR, New Delhi for the award of a Senior Research Fellowship (SRF).

References

1. Antonov, L., Kamada, K., Nedeltcheva, D., Ohta, K., Kamounah, F.S.: Gradual change of one- and two-photon absorption properties in solution—protonation of 4-N,N-dimethylamino-4′-aminoazobenzene. J. Photochem. Photobiol. A, Chem. **181**, 274–282 (2006)
2. Formosinho, S.J., Arnaut, L.G.: Excited-state proton transfer reactions. I. Fundamentals and intermolecular reactions. J. Photochem. Photobiol. A, Chem. **75**, 1–21 (1993)
3. Formosinho, S.J., Arnaut, L.G.: Excited-state proton transfer reactions. II. Intramolecular reactions. J. Photochem. Photobiol. A, Chem. **75**, 22–48 (1993)
4. O'Connor, D.B., Scott, G.W., Coulter, D.R., Yavrouln, A.: Temperature dependence of electronic energy transfer and quenching in copolymer films of styrene and 2-(2′-hydroxy-5′-vinylphenyl)-2H-benzotriazole. J. Phys. Chem. **95**, 10252–10261 (1991)
5. Chou, P.T., Martinej, M.L.: Photooxygenation of 3-hydroxyflavone and molecular design of the radiation-hard scintillator based on the excited-state proton transfer. Radiat. Phys. Chem. **41**, 373–378 (1993)
6. Nishiya, T., Ymauchi, S., Hirota, N., Baba, M., Hamazaki, I.: Fluorescence studies of intramolecularly hydrogen-bonded o-hydroxyacetophenone, salicylamide, and related molecules. J. Phys. Chem. **90**, 5730–5735 (1986)
7. Das, S.K., Dogra, S.K.: Excited state intramolecular proton transfer of 2-(2′-hydroxyphenyl)-benzimidazole in non-ionic micelles. J. Chem. Soc. Faraday Trans. I **94**, 139–145 (1998)
8. Szejtli, J., Osa, T.: In: Atwood, J.L., Davies, J.E., Mac Nicol, D.D., Vogtle, F. (eds.) Comprehensive Supramolecular Chemistry, vol. 3. Pergamon/Elsevier, Oxford (1996)
9. Meo, P.L., D'Anna, F., Riela, S., Gruttadauria, M., Noto, R.R.: Spectrophotometric study on the thermodynamics of binding of α- and β-cyclodextrin towards some p-nitrobenzene derivatives. Org. Biomol. Chem. **1**, 1584–1590 (2003)
10. Takei, M., Yui, H., Hirose, Y., Sawada, T.: Femtosecond time-resolved spectroscopy of photoisomerization of methyl orange in cyclodextrins. J. Phys. Chem. A **105**, 11395–11399 (2001)
11. Bortolus, P., Monti, S.: Cis-trans photoisomerization of azobenzene-cyclodextrin inclusion complexes. J. Phys. Chem. **91**, 5046–5050 (1987)
12. Yoshida, N., Yamauchi, H., Higashi, M.: Dynamic aspects in host–guest interactions. Kinetics of the metal complexation reactions of 2-(5-bromo-2-pyridylazo)-5-(*n*-propyl-*n*-sulfopropylamino) phenol associated with cyclodextrin inclusion reactions. J. Phys. Chem. **102**, 1523–1529 (1998)
13. Sanchez, A.M., de Rossi, R.H.: Effect of β-cyclodextrin on the thermal cis–trans isomerization of azobenzenes. J. Org. Chem. **61**, 3446–3451 (1996)
14. Abou-Hamdan, A., Bugnon, P., Saudan, C., Lye, P.G., Merbach, A.E.: High-pressure studies as a novel approach in determining inclusion mechanisms: thermodynamics and kinetics of the host–guest interactions for α-cyclodextrin complexes. J. Am. Chem. Soc. **122**, 592–602 (2000)
15. Ueno, A., Kuwabara, T., Nakamura, A., Toda, F.: A modified cyclodextrin as a guest responsive colour-change indicator. Nature **356**, 136–137 (1992)
16. Kuwabara, T., Aoyagi, T., Takamura, M., Matsushita, A., Nakamura, A., Ueno, A.: Heterodimerization of dye-modified cyclodextrins with native cyclodextrins. J. Org. Chem. **67**, 720–725 (2002)
17. Jorgenson, M.J., Horter, D.R.: A Critical re-evaluation of the Hammett acidity function at moderate and high acid concentrations of sulfuric acid. New H_0 values based solely on a set of primary aniline indicators. J. Am. Chem. Soc. **85**, 878–887 (1963)
18. Yagil, G.: The effect of ionic hydration on rate and equilibrium in concentrated electrolyte solutions. IV. The effect of neutral electrolytes on the indicator acidity of an alkaline solution. J. Phys. Chem. **71**, 1045–1052 (1967)
19. Stalin, T., Rajendiran, N.: Intra molecular charge transfer effects on 3-aminobenzoic acid. Chem. Phys. **322**, 311–322 (2006)
20. Stalin, T., Rajendiran, N.: Intramolecular charge transfer effect associated with hydrogen bonding on 2-aminobenzoic acid. J. Photochem. Photobiol. A, Chem. **182**, 137–150 (2006)
21. Stalin, T., Rajendiran, N.: Solvatochromism prototropism and complexation of *para*-aminobenzoic acid. J. Incl. Phenom. Macrocycl. Chem. **55**, 21–29 (2006)

22. Prabhu, A.A.M., Rajendiran, N.: Unusual spectral shifts on fast violet-B and benzanilide: effect of solvents, pH and β-cyclodextin. Spectrochim. Acta **74**, 484–497 (2009)
23. Stalin, T., Rajendiran, N.: Photophysical behavior of 4-hydroxy-3,5-dimethoxybenzoic acid in different solvents pH and β-cyclodextrin. J. Photochem. Photobiol. A, Chem. **177**, 144–155 (2006)
24. Stalin, T., Rajendiran, N.: Photophysical properties of 4-hydroxy-3-methoxy benzoic acid. J. Mol. Struct. **794**, 35–45 (2006)
25. Prabhu, A.A.M., Rajendiran, N.: Intra molecular proton transfer effects on 2,6-diaminopyridine. J. Fluoresc. **20**, 43–54 (2010)
26. Prabhu, A.A.M., Rajendiran, N.: Azo-ammonium tautomerism and assembly behavior of inclusion complexes of β-cyclodextrin with 4-amino, 2′,3-dimethylazobenzene and 4-amino azobenzene. Ind. J. Chem. A **49**, 407–417 (2010)
27. Joshi, H., Kamounah, F.S., van der Zwan, G., Gooijer, C., Antonov, L.: Temperature dependent absorption spectroscopy of some tautomeric azo dyes and Schiff bases. J. Chem. Soc., Perkin Trans. **2**, 2303–2308 (2001)
28. Antonov, L., Fabian, W.M.F., Nedeltcheva, D., Kamounah, F.S.: Tautomerism of 2-hydroxynaphthaldehyde Schiff bases. J. Chem. Soc., Perkin Trans. **2**, 1173–1179 (2000)
29. Smoluch, M., Joshi, H., Gerssen, A., Gooijer, C., van der Zwan, G.: Fast excited-state intramolecular proton transfer and subnanosecond dynamic Stokes shift of time-resolved fluorescence spectra of the 5-methoxysalicylic acid/diethyl ether complex. J. Phys. Chem. **109**, 535–541 (2005)
30. Alarcón, S.H., Olivieri, A.C., Labadie, G.R., Cravero, R.M., Gonzales-Sierra, M.: Tautomerism of representative aromatic—hydroxy carbaldehyde anils as studied by spectroscopic methods and AM1 calculations. Synthesis of 10-hydroxyphenanthrene-9-carbaldehyde. Tetrahedron **51**, 4619–4626 (1995)
31. Bilot, L., Kawasaki, A.: Zur Theory des Einflusses von Lösungsmitteln auf die Elektronenspektren der Molekuele. Z. Naturforsch. A **17**, 621–630 (1962)
32. Reichardt, C.: Empirical parameters of solvent polarity as linear free-energy relationships. Angew. Chem., Int. Ed. Engl. **18**, 98–110 (1979)
33. Yeh, S.J., Jaffe, H.H.: An acidity function for the solvent system consisting of 20 vol% ethanol and 80 vol% sulfuric acid–water mixtures. J. Am. Chem. Soc. **81**, 3274–3278 (1959)
34. Klotz, I.M., Fiess, H.A., Chen Ho, Y.Y., Mellody, M.: The position of the proton in substituted azobenzene molecules. J. Am. Chem. Soc. **76**, 5136–5140 (1954)
35. Strachan, W.M.J., Dolenko, A., Buncel, E.: Diprotonation equilibria involving 4-hydroxyazobenzene and 4-hydroxyazobenzene-4′-sulfonic acid. Can. J. Chem. **47**, 3631–3636 (1969)
36. Paul, M.A., Long, F.A.: H_0 and related indicator acidity function. Chem. Rev. **57**, 1–45 (1957)
37. Arnett, E.M., Wu, C.Y.: Stereoelectronic effects on organic bases. II. Base strengths of the phenolic ethers. J. Am. Chem. Soc. **82**, 5660–5665 (1960)
38. Reeves, R.L.: The protonation and indicator behavior of some ionic azobenzenes in aqueous sulfuric acid. J. Am. Chem. Soc. **88**, 2240–2247 (1969)
39. Sawcki, E.: Physical properties of the aminoazobenzene dyes. IV. The position of proton addition. J. Org. Chem. **22**, 365–367 (1957)
40. Maclean, C., Mackor, E.L.: NMR study of proton exchange of weak bases in hydrogen fluoride. Discuss. Faraday Soc. **34**, 165–176 (1962)
41. Birchall, T., Gillespie, R.J.: Nuclear magnetic resonance studies of the protonation of weak bases in fluorosulphuric acid. III. Methylbenzenes and anisole. Can. J. Chem. **42**, 502–513 (1964)
42. Birchalla, T., Bournsr, N., Gillespie, J., Smith, P.J.: Nuclear magnetic resonance studies of the protonation of weak bases in fluorosulphuric acid. IV. Phenols and aromatic ethers. Can. J. Chem. **42**, 1433–1439 (1964)
43. Yates, K., Wai, H.: The ionization of some typical weak bases in concentrated perchloric acid. Can. J. Chem. **43**, 2131–2133 (1965)
44. Gold, V., Tye, F.L.: Ultra-violet absorption spectra of conjugated hydrocarbon in sulphuric acid solution. J. Chem. Soc. **01**, 2172–2180 (1952)
45. Agbaria, R.A., Uzan, B., Gill, D.: Fluorescence of 1,6-naphthalenediol with cyclodextrins. J. Phys. Chem. **93**, 3855–3859 (2010)
46. Park, H.R., Mayer, B., Wolschann, P., Kohler, G.: Excited-state proton transfer of 2-naphthol inclusion complexes with cyclodextrins. J. Phys. Chem. **98**, 6158–6166 (1994)
47. Benesi, H.A., Hildebrand, J.H.: A spectrophotometric investigation of the interaction of iodine with aromatic hydrocarbons. J. Am. Chem. Soc. **71**, 2703–2707 (1949)
48. Rekhasky, M.V., Inoue, Y.: Complexation thermodynamics of cyclodextrins. Chem. Rev. **98**, 1875–1918 (1998)
49. Liu, Y., Zhao, Y-L., Chen, Y., Guo, D.S.: Assembly behavior of inclusion complexes of β-cyclodextrin with 4-hydroxyazobenzene and 4-aminoazobenzene. Org. Biomol. Chem. **3**, 584–591 (2005)

50. Schneider, H.J., Hacket, F., Rudiger, V., Ikeda, H.: NMR studies of cyclodextrins and cyclodextrin complexes. Chem. Rev. **98**, 1755–1786 (1998)
51. Schuette, J.M., Ndou, T., Munozde le pina, A., Greene, K.L., Werner, I.M.: Characterization of the β-cyclodextrin/acridine complex. J. Phys. Chem. **95**, 4897–4902 (1991)
52. Smith, V.K., Nodu, T.T., Werner, I.M.: Spectroscopic study of the interaction of catechin with α-, β-, and γ-cyclodextrins. J. Phys. Chem. **98**, 8627–8631 (1994)
53. CAChe reference, version 7.5, Fujitsu Limited CAChe Oxford Molecular Ltd. (2002); CAChe Guide to MOPAC, version 7.5, Fujitsu Limited CAChe Oxford Molecular Ltd. (2002)
54. Das, S.K.: Inclusion complexation of 2-(4′-*N*,*N*-dimethylaminophynyl)-*1H*-naphth[2,3-d]imidazole by β-cyclodextrin: effect on the TICT emission. Chem. Phys. Lett. **361**, 21–28 (2002)
55. Balamurali, M.M., Dogra, S.K.: Intra and intermolecular proton transfer in methyl-2-hydroxy nicotinate. J. Lumin. **110**, 147–163 (2004)